Inorg. Chem. **2006**, *45*, 4071−4078

A New Family of Mono- and Dicarboxylic Ruthenium Complexes $[Ru(DIP)_2(L_2)]^{2+}$ (DIP = 4,7-diphenyl-1,10-phenanthroline): Synthesis, Solution Behavior, and X-ray Molecular Structure of *trans*-$[Ru(DIP)_2(MeOH)_2][OTf]_2$

Regis Caspar,[†] Christine Cordier,[‡] Jenny B. Waern,[†] Carine Guyard-Duhayon,[†] Michel Gruselle,[†] Pascal Le Floch,[§] and Hani Amouri*,[†]

Laboratoire de Chimie Inorganique et Matériaux Moléculaires, UMR CNRS 7071, Université Pierre et Marie Curie Paris VI, 4 place Jussieu, case 42, 75252 Paris Cedex 05, France, ITODYS, UMR CNRS 7086, Université Paris 7, Denis Diderot, 1 rue Guy de la Brosse, 75005 Paris, France, and Laboratoire "Hétéroéléments et Coordination", UMR CNRS 7653 (DCPH), Département de Chimie, Ecole Polytechnique, 91128 Palaiseau Cédex, France

Received January 20, 2006

A new family of ruthenium complexes of general formula $[Ru(DIP)_2(L_2)]^{2+}$, where DIP = 4,7-diphenyl-1,10-phenanthroline, a bidentate ligand with an extended aromatic system, was prepared and fully characterized. When L is a monodentate ligand, the following complexes were obtained: L = $CF_3SO_3^{-1}$ (**2**), CH_3CN (**3**), and MeOH (**4**). When L_2 is a bidentate ligand, the compounds $[Ru(DIP)_2(Hcmbpy)][Cl]_2$ (**5**) and $[Ru(DIP)_2(H2dcbpy)][Cl]_2$ (**6**) were prepared (Hcmbpy = 4-carboxy-4′-methyl-2,2-bipyridine, H2dcbpy = 4,4′-dicarboxy-2,2′-bipyridine). Complex $[Ru(DIP)_2(MeOH)_2][OTf]_2$ (**4**) displayed a trans configuration of the DIP ligands, which is rare for octahedral complexes featuring DIP bidentate ligands. DFT calculations carried out on **4** showed that the cis isomer is more stable by 12.2 kcal/mol relative to the trans species. The solution behaviors of monocarboxylic complex $[Ru(DIP)_2(Hcmbpy)][Cl]_2$ (**5**) and dicarboxylic complex $[Ru(DIP)_2(H2dcbpy)][Cl]_2$ (**6**) were investigated by ^1H NMR spectroscopy. VT-NMR, concentration dependence, and reaction with NaOD allowed us to suggest that aggregation of the cationic species in solution, especially for **6**, originates mainly from hydrogen bonding interactions.

Introduction

Among the most important types of noncovalent interactions in solutions encountered in both biological and chemical systems are hydrogen-bonding and $\pi-\pi$ interactions.[1] A remarkable example provided by nature is DNA, which has a double helical structure that involves two complementary strands linked together via hydrogen bonding and $\pi-\pi$ stacking interactions.[2] Furthermore, these two interactions are of pivotal importance in the construction of supermolecules through supramolecular assembly.[1,3] The field of coordination chemistry provides an opportunity to study these interactions through the design of complexes incorporating both π-stacking and hydrogen-bonding functionalities. In 1984, Yamatera and co-workers showed by ^1H NMR studies that complex $[Ru(phen)_3]^{2+}$ displays self-association in solution.[4] In aqueous media, this species gives rise to NMR spectra that are significantly concentration-dependent and display features consistent with π-stacking interactions between cations to form dimers (Figure 1).

More recently, it has been shown by NMR and X-ray crystallography that the octahedral eilatin complexes $[M(L-L)_2(eilatin)]^{2+}$ (M = Ru, Os; L−L = bpy, phen), where eilatin is a heptacyclic aromatic ligand with strong π-character, dimerize in solution via $\pi-\pi$ stacking.[5] In particular, the X-ray crystallography showed that a hetero-

* To whom correspondence should be addressed. E-mail: amouri@ccr.jussieu.fr.
[†] Université Pierre et Marie Curie Paris VI.
[‡] Université Paris 7.
[§] Ecole Polytechnique.

(1) Steed, J. W.; Atwood, J. L. *Supramolecular Chemistry*; Wiley: Chichester, U.K., 2000.
(2) (a) Watson, J. D.; Crick, F. H. C. *Nature* **1953**, *171*, 737−738. (b) Calladine, C. R.; Drew, H. R. *Understanding DNA: The Molecule and How It Works*, 2nd ed.; Academic Press: New York, 1997.
(3) Lehn, J.-M. *Supramolecular Chemistry, Concept and Perspectives*; VCH: Weinheim, Germany, 1995.
(4) Masuda, Y.; Yamatera, H. *Bull. Chem. Soc. Jpn.* **1984**, *57*, 58−62.

10.1021/ic0601236 CCC: $33.50
Published on Web 04/14/2006

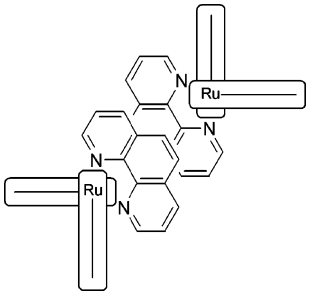

Figure 1. Schematic representation of $[Ru(phen)_3]^{2+}$ showing π-stacking interactions between bidentate phenanthroline ligands, giving rise to dimers in solution.

chiral association is formed between Δ-$[M(L-L)_2(eilatin)]^{2+}$ and Λ-$[M(L-L)_2(eilatin)]^{2+}$ cations. All of the examples reported so far have focused on complexes with ligands incorporating only π-stacking functionalities. Thus, octahedral metal complexes with ligands displaying both hydrogen-bonding and $\pi-\pi$ interactions have not been investigated, to the best of our knowledge. To this end, we report here the synthesis of some ruthenium polypyridyl complexes of general formula $[Ru(DIP)_2(L_2)][Cl]_2$, where DIP = 4,7-diphenylphenanthroline, a strong π-character ligand, and L_2 = Hcmbpy = 4-carboxy-4′methyl-2,2′-bipyridine (**5**) and H2dcbpy = 4,4′-dicarboxy-2,2′-bipyridine (**6**). Both ligands possess carboxylic acid groups and are therefore capable of hydrogen bonding. The solution behavior of these compounds was studied by NMR spectroscopy, providing valuable information about the nature of the interaction between cations in solution. We also report the synthesis and full characterization of novel complexes $[Ru(DIP)_2(OTf)_2]$ (**2**) and $[Ru(DIP)_2(CH_3CN)_2][OTf]_2$ (**3**). Furthermore, the synthesis and X-ray molecular structure of *trans*-$[Ru(DIP)_2(MeOH)_2][OTf]_2$ (**4**) are included.

Results and Discussion

In a previous work, we reported the enantioselective synthesis of the ruthenium complexes with mixed bipyridyl ligands, (Δ, Λ)-$[Ru(bpy)_2(Hcmbpy)][PF_6]_2$ and (Δ, Λ-$[Ru(bpy)_2$-(H2dcbpy)$][PF_6]_2$, where one of the bipyridyl ligands carries either one or two carboxylic functionalities.[6] The monocarboxylic compounds showed moderate binding to DNA, and the dicarboxylic Δ-$[Ru(bpy)_2(H2dcbpy)][PF_6]_2$ cleaved DNA.[7]

Pursuing our research in this area, we intended to prepare the analogous compounds using a strong π-acceptor ligand such as DIP = 4,7-diphenylphenanthroline instead of bpy = bipyridine. Our choice of this ligand stems from the fact that other groups have shown that complexes such as $[Ru(phen)_2(L_2)]^{2+}$, where L_2 is a polypyridyl ligand with a strong π-acceptor character, show strong binding to DNA and intercalate between DNA base pairs.[8] Complexes with mixed bipyridyl ligands are well-known; in contrast, complexes with mixed DIP ligands have been less fully investigated. We note, however, that complex $[Ru(DIP)_3][Cl]_2$ has been fully characterized and examined by several groups.[9]

Chart 1

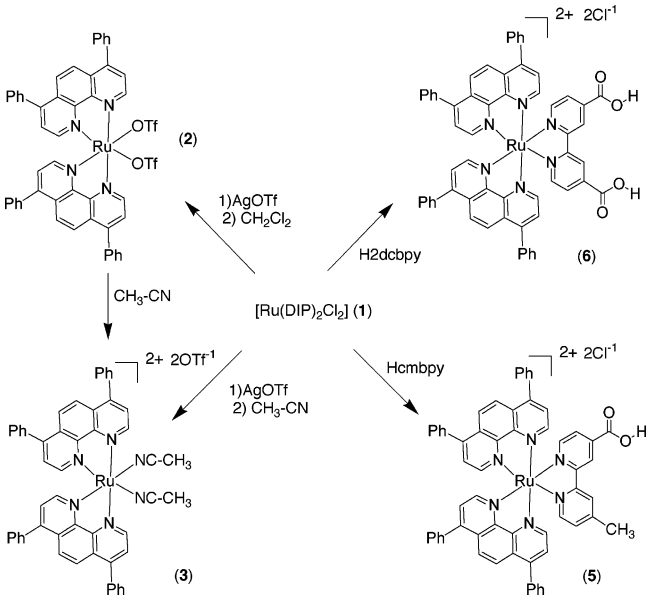

Treatment of $RuCl_3 \cdot nH_2O$ with 2 equiv of DIP in distilled DMF provided chloride derivative $[Ru(DIP)_2Cl_2]$ (**1**) as violet microcrystalline material in 71% yield. When $[Ru(DIP)_2Cl_2]$ (**1**) was treated with AgOTf in CH_2Cl_2, the dark burgundy complex $[Ru(DIP)_2(OTf)_2]$ (**2**) was obtained in 94% yield (Chart 1). This complex was fully characterized by elemental analysis and NMR spectroscopy. The infrared spectrum of **2** recorded from KBr disks showed bands characteristic of coordinated triflates ν(SO) at 1023 and 1308 cm^{-1} and $\nu(CF_3)$ at 1166 and 1235 cm^{-1}, which are at lower wavenumbers than for uncoordinated triflates.[10] The reaction of **2** with CH_3CN for 24 h proceeded smoothly at room temperature and provided a microcrystalline bright orange compound in 93% yield, which was fully characterized and gave spectroscopic and analytical data consistent with $[Ru(DIP)_2(CH_3CN)_2][OTf]_2$ (**3**) (Chart 1). The ^1H NMR spectrum showed one singlet at δ 2.53 for the two coordinated CH_3CN molecules, which integrated to six protons. Complexes **2** and **3** are stable in air and can be stored for long periods of time. Attempts to obtain target complexes $[Ru(DIP)_2(Hcmbpy)][Cl]_2$ (**5**) and $[Ru(DIP)_2(H2dcbpy)][Cl]_2$ (**6**) from either complex have been unsuccessful. This indicates that the binding of either the CH_3CN or the triflate anion to the ruthenium center is not labile. This is in contrast to the usual behavior of triflate anions, which are considered to be weakly binding anions.[10] It may be that the steric and

(5) (a) Gut, D.; Rudi, A.; Kopilov, J.; Goldberg, I.; Kol, M. *J. Am. Chem. Soc.* **2002**, *124*, 5449−5456. (b) Bergman, S. D.; Kol, M. *Inorg. Chem.* **2005**, *44*, 1647−1654.
(6) Caspar, R.; Amouri, H.; Gruselle, M.; Cordier, C.; Malézieux, B.; Duval, R.; Lévêque, H. *Eur. J. Inorg. Chem.* **2003**, 499−505.
(7) Caspar, R.; Musatkina, L.; Tatosyan, A.; Amouri, H.; Gruselle, M.; Guyard-Duhayon, C.; Duval, R.; Cordier, C. *Inorg. Chem.* **2004**, *43*, 7986−7993.
(8) Erkkila, K. E.; Odom, D. T.; Barton, J. K. *Chem. Rev.* **1999**, *99*, 2777−2796 and references therein.
(9) (a) Goldstein, B. M.; Barton, J. K.; Berman, H. M. *Inorg. Chem.* **1986**, *25*, 842−847. (b) Kim, H.-K.; Lincoln, P.; Nordén, B.; Tuite, E. *Chem. Commun.* **1997**, 2375−2376.
(10) Mahon, M. F.; Whittlesey, M. K.; Wood, P. T. *Organometallics* **1999**, *18*, 4068−4074.

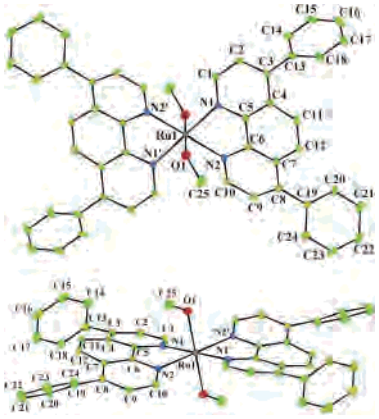

Figure 2. Top: X-ray molecular structure of the cation of **4**, *trans*-[Ru(DIP)$_2$(MeOH)$_2$]$^{2+}$, with hydrogen atoms omitted. The thermal ellipsoids correspond to the 30% probability level. Bottom: alternative view of the cation of **4**, perpendicular to the plane of the methanol molecules. Selected bond distances (Å) and angles (deg): Ru1···N1 = 2.075(4), Ru1···N2 = 2.077(4), Ru1···O1 = 2.090(4), C1···N1 = 1.336(7), N1···C5 = 1.371(6), C5···C6 = 1.427(7), N2···C6 = 1.372(6), N2···C10 = 1.327(7), C1···C2 = 1.399(7), C2···C3 = 1.388(8), C3···C4 = 1.426(7), C4···C11 = 1.437(7), C11···C12 = 1.343(8), C7···C12 = 1.438(7), C7···C8 = 1.430(8), C8···C9 = 1.386(8), C9···C10 = 1.394(7), O1···C25 = 1.433(8). N1···Ru1···N2 = 78.14(17), N1···Ru1···N2′ = 101.86(17), N1···Ru1···O1 = 89.26(17), N2···Ru1···O1 = 90.05(17), N1···C5···C6 = 115.7(4), N2···C6···C5 = 115.7(4).

electronic effects of the DIP ligands in **2** render the triflate anions less labile.

Compounds **2** and **3** were highly soluble in most organic solvents, which prevented the preparation of crystals of either complex for an X-ray study. However, very few crystals were obtained after the diffusion of diethyl ether into a methanol solution of **2** over several weeks. A single-crystal X-ray diffraction study was undertaken and gave an X-ray molecular structure identified unexpectedly as *trans*-[Ru(DIP)$_2$(MeOH)$_2$][OTf]$_2$ (**4**). Although **4** was first obtained unintentionally, it was later formed reproducibly, always in small amounts upon the attempted crystallization of *cis*-[Ru(DIP)$_2$(OTf)$_2$] (**2**) from MeOH/Et$_2$O, which remained in solution.

X-ray Molecular Structure of Trans-[Ru(DIP)$_2$(MeOH)$_2$][OTf]$_2$ (4). Complex **4** crystallizes in the monoclinic unit cell with space group *P*2/*n*. A view of the cationic part with atom labeling and selected bond distances and angles are shown in Figure 2. The structure shows the presence of two bidentate DIP ligands occupying the equatorial positions in a trans geometry. The two coordinated MeOH molecules are in the axial positions, completing the octahedral geometry around the metal center. The phenanthroline unit of the DIP ligand is planar, whereas the two phenyl groups deviate out of the plane by a dihedral angle of almost 45°. The Ru−N bond distance is 2.07−2.08 Å, slightly longer than that reported for the [Ru(DIP)$_3$][Cl]$_2$ complex with Ru−N = 2.06 Å[9a] and shorter than that reported for [Ru([9]aneS$_3$)(DIP)Cl][BF$_4$] with Ru−N = 2.10 Å.[11] The bite angle N−Ru−N of DIP in **4** is 78°, slightly smaller than that reported for [Ru(DIP)$_3$][Cl]$_2$, about 79−81°,[9a] and that reported for [Ru([9]aneS$_3$)(DIP)Cl][BF$_4$], 79°.[11] Although some trans complexes of ruthenium bipyridyl and ruthenium phenanthroline have been reported,[12] to the best of our knowledge, trans-[Ru(DIP)$_2$(MeOH)$_2$][OTf]$_2$ (**4**) is the first X-ray structure of a ruthenium complex with two DIP ligands in trans position. Furthermore, several *trans*-ruthenium polypyridyl complexes have been reported that incorporate rigid tetradentate chelating ligands that force the four nitrogen atoms to occupy the equatorial positions, leaving the coordinated solvents on the axial position.[13] It is clear that these examples, in which the tetradentate ligands are able to adopt only the trans configuration, are intrinsically different from our *trans*-ruthenium complex [Ru(DIP)$_2$(MeOH)$_2$][OTf]$_2$ (**4**) that features bidentate ligands, for which the preferred geometry is cis. In summary, a trans configuration for **4** is a rare example of this geometry of the DIP ligands in the literature.

Cis−trans Isomerization and Computational Study. The unexpected formation of *trans*-[Ru(DIP)$_2$(MeOH)$_2$][OTf]$_2$ (**4**) from a solution of *cis*-[Ru(DIP)$_2$(OTf)$_2$] (**2**) during crystallization from MeOH/Et$_2$O prompted us to study this behavior experimentally and by computation (vide infra). The ^{1}H NMR of **4** recorded in CD$_2$Cl$_2$ showed the presence of only five sets of signals, consistent with a higher symmetry (trans configuration) than that of complex **2** (*cis* configuration); interestingly, the bound methanol molecules gave rise to a singlet at δ 3.46 and integrated to six protons. We note that *trans*-[Ru(DIP)$_2$(MeOH)$_2$][OTf]$_2$ (**4**) was unstable in solution and decomposed slowly. In contrast, on leaving **2** in CD$_3$OD for a period of 1 month, we detected no decomposition or signals corresponding to **4**. Indeed, previous experimental work shows preferential formation of the cis isomer, and the interconversion to the trans isomer appears difficult to achieve.[14] Thus, we performed a computational study within the framework of DFT using the Gaussian set of programs. Calculations were performed using the B3PW91 functional (see Experimental Section for further details regarding basis sets employed and methods). In a first series of calculations, the phenyl groups were replaced by H atoms and the cis and trans configurations of the related complex [Ru(phen)$_2$(MeOH)$_2$]$^{2+}$ were optimized. Both calculations yielded structures that are very close to the experimental ones. The energies obtained for both configurations suggest that the cis isomer is more stable by 13.6 kcal/mol relative to the trans species. To get more accurate data, we carried out calculations on the complexes featuring phenyl groups. The ONIOM (B3PW91/UFF) method was employed to minimize computation time. Only the phenyl groups were computed at the molecular mechanics level of theory, with the core of the complex (the two phen and two MeOH ligands as well as the Ru atom) being computed at the

(11) Madureira, J.; Santos, T. M.; Goodfellow, B. J.; Lucena, M.; Pedrosa de Jesus, J.; Santana-Marques, M. G.; Drew, M. G. B.; Félix, V. *J. Chem. Soc., Dalton Trans.* **2000**, 4422−4431.

(12) (a) Coe, B. J.; Meyer, T. J.; White, P. S. *Inorg. Chem.* **1993**, *32*, 4012−4020. (b) Nazeeruddin, M. K.; Zakeeruddin, S. M.; Humphry-Baker, R.; Gorelsky, S. I.; Lever, A. B. P.; Gratzel, M. *Coord. Chem. Rev.* **2000**, *208*, 213−225. (c) Bonneson, P.; Walsh, J. L.; Pennington, W. T.; Cordes, A. W.; Durham, B. *Inorg. Chem.* **1983**, *22*, 1761−1765.

(13) (a) Renouard, T.; Fallahpour, R.-A.; Nazeeruddin, M. K.; Humphry-Baker, R.; Gorelsky, S. I.; Lever, A. B. P.; Gratzel, M. *Inorg. Chem.* **2002**, *41*, 367−378. (b) Concepcion, J.; Just, O.; Laiva, A. M.; Loeb, B.; Ress, W. S. *Inorg. Chem.* **2002**, *41*, 5937−5939.

(14) Concepcion, J.; Loeb, B.; Simon-Manso, Y.; Zuloaga, F. *Polyhedron* **2000**, *19*, 2297−2302.

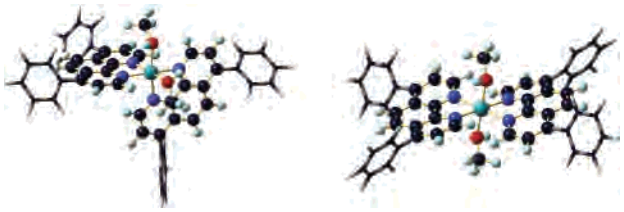

Figure 3. Optimized structure of the real complexes computed at the ONIOM (B3PW91:UFF) level of theory (cis complex on the left and trans complex on the right-hand side). Atoms included in the QM part are shown in ball-and-stick format, and atoms included in the MM part are represented by tubes.

quantum mechanics level of theory. Here again, a good fit between experimental and theoretical structures was obtained. Single-point calculations were carried out on the ONIOM structures at the quantum mechanics level of theory (using the same basis sets as those used for the calculations on the model complexes). Views of the two optimized structures are shown in Figure 3. Interestingly, we found that the introduction of phenyl groups does not significantly modify the energy difference between the two configurations, and the cis isomer was found to be more stable by 12.2 kcal/mol relative to the trans species.

These results support our experimental findings on the instability of **4** in solution. We believe that the trans isomer of **2** is formed in small amounts during the preparation of compound **2** but in low quantities (less than 5%) by analysis of the ^{1}H NMR spectrum of **2**. Another possible explanation is photochemical transformation of *cis*-**2** to *trans*-**4** during the crystallization process of **2**.

Preparation of Target Complexes [Ru(DIP)$_2$(Hcmbpy)][Cl]$_2$ (5) and [Ru(DIP)$_2$(H2dcbpy)][Cl]$_2$ (6) and Solution Behavior. Treatment of [Ru(DIP)$_2$Cl$_2$] (**1**) with either monocarboxylic-bpy (Hcmbpy) or dicarboxylic-bpy (H2dcbpy) in a MeOH/H_2O mixture provided complexes [Ru(DIP)$_2$(Hcmbpy)][Cl]$_2$ (**5**) and [Ru(DIP)$_2$(H2dcbpy)][Cl]$_2$ (**6**) in 92 and 96% yield, respectively. Complex **5** was obtained as a red microcrystalline material, whereas **6** was obtained as a burgundy powder. Both compounds were fully characterized by spectroscopic methods and elemental analysis.

Complexes [Ru(DIP)$_2$(Hcmbpy)][Cl]$_2$ (**5**) and [Ru(DIP)$_2$(H2dcbpy)][Cl]$_2$ (**6**) were highly soluble in many organic solvents, but the ^{1}H NMR spectra obtained from different solutions were markedly different. For instance, the ^{1}H NMR spectra obtained from a 3 mM solution of either **5** or **6** in CD_3CN or DMSO-d_6 at 295 K showed sharp, clearly resolved peaks, whereas a similar solution in CD_2Cl_2 showed broadened peaks for **5** and extremely broad signals for **6**. Such behavior has been observed for octahedral ruthenium complexes with bidentate ligands that possess extended aromatic systems and has been attributed to the aggregation of cationic species in solution through $\pi-\pi$ interactions.[4,5] However, our complexes incorporate both carboxylic acid groups, which are capable of displaying hydrogen bonding, and extended aromatic systems, which can display π-stacking behavior, and hence the aggregation in solution may result from either interaction or a combination of both interactions. Thus, we carried out several ^{1}H NMR experiments in order to elucidate the nature of the aggregation interaction.

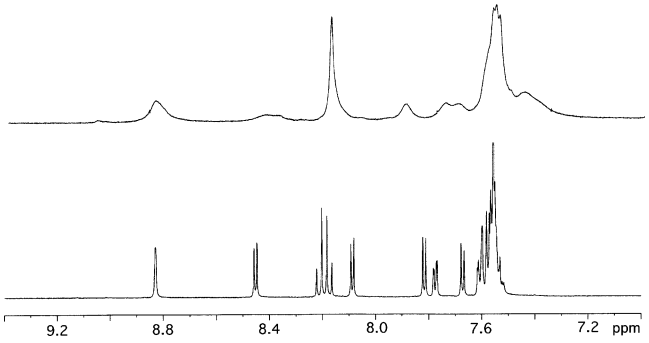

Figure 4. ^{1}H NMR spectra (500 MHz) of [Ru(DIP)$_2$(H2dcbpy)][Cl]$_2$ (**6**) in CD_2Cl_2 without NaOD (upper trace) and after the addition of NaOD (lower trace).

(i) Temperature Dependence. Variable-temperature (VT) NMR studies of **6** were conducted in $C_2D_2Cl_4$ (bp 145 °C) in the range 293−353 K. Upon warming the sample, we observed some improvement in resolution. However, at 353 K, the maximum temperature investigated, the peaks remained broad and poorly resolved, suggesting that strong aggregation occurs among individual cations in this solvent. Analogous experiments were performed in CD_3CN, because the resolved signals in this solvent could be assigned. Increasing the temperature of a 3 mM solution of **5** or **6** in CD_3CN resulted in no significant changes in resolution or line widths. However, the proton H3 adjacent to the carboxylic group in [Ru(DIP)$_2$(Hcmbpy)][Cl]$_2$ (**5**) underwent a downfield shift of approximately 0.1 ppm when the temperature was raised to 333 K. The spectrum of complex **6** showed changes in the same peaks as for **5** but to a lesser extent. The maximum change in chemical shift observed for H3 in [Ru(DIP)$_2$(H2dcbpy)][Cl]$_2$ (**6**) was approximately 0.03 ppm.

(ii) Concentration Dependence. The effect of concentration on the ^{1}H NMR spectra of both complexes was also studied in CD_3CN solution, with results similar to those from the temperature-dependence experiments. With a change in concentration from 3 to 0.3 mM [Ru(DIP)$_2$Hmcbpy][Cl]$_2$, the ^{1}H NMR spectra showed several small changes in the chemical shifts of several peaks. Again, the largest change was for H3, which underwent a total shift of approximately 0.03 ppm over this concentration range. The [Ru(DIP)$_2$(H2dcbpy)][Cl]$_2$ (**6**) complex showed negligible changes with the 10-fold lower concentration in CD_3CN.

(iii) Addition of NaOD. The most striking ^{1}H NMR spectral changes were obtained when NaOD (5 equiv) was added to a 2.7 mM solution of either complex **5** or **6** in CD_2Cl_2. An immediate and dramatic sharpening of all the peaks in the spectrum of both [Ru(DIP)$_2$(Hmcbpy)][Cl]$_2$ (**5**) and [Ru(DIP)$_2$(H2dcbpy)][Cl]$_2$ (**6**) was observed. The result was particularly significant for the diacidic [Ru(DIP)$_2$(H2dcbpy)][Cl]$_2$ complex (Figure 4), for which the ^{1}H NMR spectrum displayed the most broadening prior to the addition of the NaOD.

In addition to the sharpening and resolution of the peaks in the spectra of [Ru(DIP)$_2$(Hcmbpy)][Cl]$_2$ (**5**), changes in the chemical shifts were also observed, so that most of the peaks underwent chemical shift changes of approximately

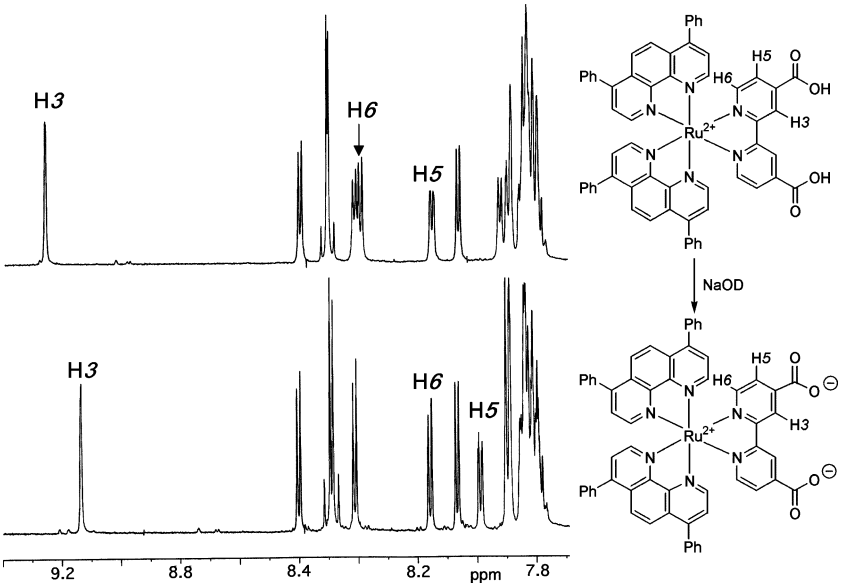

Figure 5. ^{1}H NMR spectra (500 MHz) of [Ru(DIP)$_2$(H2dcbpy)][Cl]$_2$ (**6**) in MeOH-d_4 of **6** (upper trace) and after the addition of NaOD (lower trace).

0.1 ppm. The chemical shift changes due to the addition of NaOD are difficult to analyze in the spectra of [Ru(DIP)$_2$-(H2dcbpy)][Cl]$_2$ (**6**) (Figure 4), because of the extent of the broadening in the spectrum of the CD_2Cl_2 solution. However, it appears that significant changes in the chemical shifts of several peaks occurred with the addition of NaOD.

The changes in chemical shift after NaOD addition to [Ru(DIP)$_2$(H2dcbpy)][Cl]$_2$ (**6**) were therefore analyzed in MeOH-d_4, because the peaks in this solvent were well-resolved both before and after the addition of NaOD and hence could be unambiguously assigned. As expected, the largest changes in chemical shifts were observed for the protons situated on the dicarboxylic-bpy (H2dcbpy) unit of complex **6**. In contrast, little change was seen for the protons situated on the DIP bidentate ligands. For instance, protons H3 and H5, situated ortho to the carboxylate groups, underwent upfield shifts of 0.12 and 0.17 ppm, respectively, upon the addition of 5 equiv of NaOD; proton H6, situated meta to the carboxylate groups and in the ortho position to the heterocyclic nitrogen, underwent an upfield shift of 0.24 ppm (Figure 5).

These experiments show clearly that aggregation observed for **5** and **6** in CD_2Cl_2 solution is mainly due to strong hydrogen bonding between the individual ruthenium cations. This association is stronger in **6**, because of the presence of two carboxylic functions, than in **5**. Deprotonation by NaOD removes the hydrogen-bonding interaction and hampers the cations' association. We feel that the $\pi-\pi$ interactions in these complexes, if occurring, are much weaker than the interaction due to hydrogen bonding. In previous work, we reported the X-ray molecular structure of dicarboxylic complex [Ru(bpy)$_2$(H2dcbpy)][PF$_6$]$_2$. The structure shows the formation of a double-chained 1D polymer in which a Λ-[Ru(bpy)$_2$(H2dcbpy)]$^{2+}$ cationic subunit is connected to a Δ-[Ru(bpy)$_2$(H2dcbpy)]$^{2+}$ cationic subunit by two hydrogen bonds of equal distances, with d(O$-$O) = 2.60 Å (Figure 6).[7]

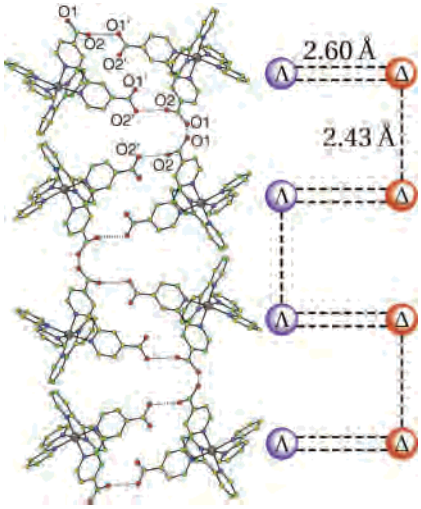

Figure 6. Double-chained 1D polymer of [Ru(bpy)$_2$(H2dcbpy)]$^{2+}$ showing hydrogen-bonding association between Δ and Λ enantiomers. From H. Amouri and C. Cordier et al. *Inorg. Chem.* **2004**, *43*, 7986. Reprinted with permission.

These heterochiral ($\Lambda-\Delta$) units are enchained through strong intermolecular hydrogen bonding in an alternate homochiral fashion with a d(O$-$O) distance of 2.43 Å (Figure 6). [Ru(DIP)$_2$(H2dcbpy)][Cl]$_2$ (**6**) is expected to show a related hydrogen-bonded structure (Figure 7). In summary, these hydrogen-bonding interactions are responsible for the association behavior observed in solution by ^{1}H NMR of **5** and **6**. It is worth mentioning that X-ray structures of octahedral metal complexes with three DIP ligands (e.g., [Ru(DIP)$_3$][Cl]$_2$[9a]) and two DIP ligands (e.g., [Os(DIP)$_2$-(Ph$_2$As$-$CH$_2-$CH$_2-$AsPh$_2$)][Ts]$_2$[15]) have been reported and showed no $\pi-\pi$ stacking interactions between the phenanthroline groups of DIP in the solid state. In contrast, a complex with one DIP ligand, [Ru([9]ane S$_3$)(DIP)Cl][BF$_4$], showed $\pi-\pi$ stacking between the phenanthroline part of

(15) Carlson, B.; Phelan, G. D.; Kaminsky, W.; Dalton, L.; Jiang, X.; Liu, S.; Jen A. K.-Y. *J. Am. Chem. Soc.* **2002**, *124*, 14162−14172.

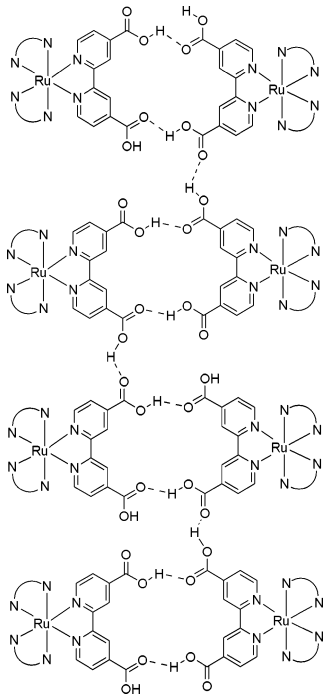

Figure 7. Proposed structure for $[Ru(DIP)_2(H2dcbpy)]^{2+}$ showing association between the individual octahedral ruthenium complexes through hydrogen bonding.

DIP.[11] By comparison, we feel that $[Ru(DIP)_2(H2dcbpy)][Cl]_2$ (**6**) will not show a $\pi-\pi$ interaction; hence, the association behavior results from hydrogen bonding. This work shows a new example in which the association of cations in octahedral metal complexes arises from hydrogen bonding and complements previous examples in octahedral ruthenium complexes in which $\pi-\pi$ stacking was responsible for their association in solution.[4,5]

Conclusion

In this paper, the synthesis of a new family of ruthenium complexes of general formula $[Ru(DIP)_2(L_2)]^{2+}$, where DIP = 4,7-diphenyl-1,10-phenanthroline, a bidentate ligand with extended aromatic system, is reported. When L is a monodentate ligand, the following complexes were obtained: L = $CF_3SO_3^{-1}$ (**2**), CH_3CN (**3**), and MeOH (**4**). Complex $[Ru(DIP)_2(MeOH)_2][OTf]_2$ (**4**) displayed a trans configuration of the DIP ligands, a rare example of this geometry in the literature. Monocarboxylic complex $[Ru(DIP)_2(Hcmbpy)][Cl]_2$ (**5**) and dicarboxylic compound $[Ru(DIP)_2(H2dcbpy)][Cl]_2$ (**6**) were also prepared, and their solution behaviors were investigated by ^1H NMR spectroscopy. VT-NMR, concentration dependence, and reaction with NaOD allowed us to suggest that aggregation of the cationic species in solution, especially for **6**, originates mainly from hydrogen-bonding interactions.

Experimental Section

All solvents used were reagent grade or better. Deuterated solvents and commercially available reagents were used as received. ^1H NMR spectra were recorded on a Bruker AC-300 spectrometer and a Bruker DRX-500 spectrometer equipped with a Silicon Graphics workstation. Chemical shifts are reported in parts per million downfield from tetramethylsilane and are referenced to the residual hydrogen signal of deuterated solvents (CHD_2CN at 1.94 ppm, CHD_2OD at 3.31 ppm, $CHDCl_2$ and C_2HDCl_4 at 5.30 ppm). NaOD experiments were carried out by the addition of NaOD (10 μL, 0.1 M solution in D_2O) to a solution of the relevant complex in the solvent indicated (500 μL), followed by shaking for 5 min. IR spectra were recorded on a Bio-RAD FTS 165 FT-IR spectrophotometer as KBr pellets in the 4000−400 cm^{-1} region.

$[Ru(DIP)_2Cl_2]$ (1). A solution of $RuCl_3 \cdot 3H_2O$ (196 mg, 0.75 mmol), Ph_2Phen (500 mg, 1.50 mmol, 2 equiv), and LiCl (223 mg, 5.4 mmol, 7.2 equiv) in DMF (15 mL) was heated to reflux for 24 h. The reaction mixture was then cooled to 4 °C, resulting in the crystallization of the product, which was filtered and washed with water and diethyl ether. A second crop was obtained after the addition of acetone to the filtrate, which was then left standing at 4 °C for 24 h. The two crops were combined and dried under vacuum to give the product (447 mg, 71%) as a microcrystalline purple powder. ^1H NMR (300 MHz, CD_2Cl_2, 298 K): δ 7.20 (2 H, d, J = 5.7 Hz), 7.48 (10 H, d, J = 5.3 Hz), 7.65 (6 H, m), 7.78 (4 H, dd, J = 1.8, 6.6 Hz), 8.03 (6 H, m), 8.17 (2 H, d, J = 9.5 Hz), 10.63 (2 H, d, J = 5.3 Hz). ^{13}C NMR (125 MHz, CD_2Cl_2, 293 K): δ 126.24 (CH), 126.45 (CH), 127.11 (CH), 127.31 (CH), 128.40 (CH), 128.73 (quat), 129.14 (quat), 129.50 (CH), 129.58 (CH), 130.04 (CH), 130.12 (CH), 130.32 (CH), 130.67 (CH), 136.00 (quat), 136.27 (quat), 138.33 (CH), 149.06 (quat), 149.29 (quat), 149.32 (quat), 149.60 (quat), 154.36 (CH), 154.53 (CH), 154.67 (CH). IR (KBr disk): υ 668, 702, 735, 766, 830, 847, 913, 1026, 1086, 1252, 1399, 1414, 1443, 1491, 1507, 1671, 1968, 2927, 3056 cm^{-1}. Anal. Calcd. for $C_{48}H_{32}Cl_2N_4Ru \cdot DMF \cdot H_2O$: C, 66.02; H, 4.45; N, 7.55. Found: C, 65.87; H, 4.66; N, 7.53.

$[Ru(DIP)_2(OTf)_2]$ (2). A solution of $[Ru(DIP)_2Cl_2] \cdot DMF \cdot H_2O$ (100 mg, 0.11 mmol) in CH_2Cl_2 (20 mL) was added to AgOTf (64 mg, 0.25 mmol, 2.3 equiv). The solution immediately turned from purple to red and was stirred for 24 h in the dark. The reaction mixture was then filtered through Celite, and the solution volume was concentrated to approximately 3 mL by evaporation of the solvent. The addition of diethyl ether resulted in the precipitation of the product, which was filtered and dried under vacuum to give the product (108 mg, 94%) as a microcrystalline dark red powder. ^1H NMR (300 MHz, CD_3OD, 298 K): δ 7.47 (2 H, d, J = 5.7 Hz), 7.54 (10 H, s), 7.71 (6 H, m), 7.90 (4 H, d, J = 6.9 Hz), 8.09 (2 H, d, J = 5.6 Hz), 8.18 (2 H, d, J = 9.4 Hz), 8.35 (2 H, d, J = 7.7 Hz), 8.37 (2 H, d, J = 3.7 Hz), 9.95 (2 H, d, J = 5.4 Hz). IR (KBr disk): υ 517, 637, 702, 741, 764, 838, 849, 1023 (SO_3), 1166, 1212, 1235, 1262 (C−F), 1308, 1397, 1420, 1447, 1559, 1594, 1625, 1652, 2817, 2848, 2929, 2953, 2972, 3061, 3103 cm^{-1}. Anal. Calcd. for $C_{50}H_{32}F_6N_4O_6RuS_2 \cdot 5CH_2Cl_2$: C, 44.37; H, 2.84; N, 3.76. Found: C, 44.45; H, 2.83; N, 4.44.

$[Ru(DIP)_2(MeCN)_2][OTf]_2$ (3). A solution of $[Ru(DIP)_2Cl_2] \cdot DMF \cdot H_2O$ (305 mg, 0.33 mmol) in CH_2Cl_2 (50 mL) was added to AgOTf (248 mg, 0.97 mmol, 2.9 equiv) under Ar. The solution immediately turned from purple to red and was stirred for 24 h in the dark. The reaction mixture was then filtered through Celite, and the solvent was removed by evaporation. Acetonitrile (45 mL) was added to the residue, and the mixture was stirred for 24 h under Ar. The solution volume was concentrated to approximately 3 mL by evaporation of the solvent, and the addition of diethyl ether resulted in the precipitation of the product, which was filtered and dried under vacuum to give the product (353 mg, 93%) as a microcrystalline orange powder. ^1H NMR (500 MHz, CD_2Cl_2, 303 K): δ 2.53 (6 H, s, MeCN), 7.54 (6 H, d, J = 5.9 Hz, H3, H22, H26), 7.60 (6 H, d, J = 6.5 Hz, H23, H24, H25), 7.72 (2 H, d, J = 7.2 Hz, H18), 7.76 (4 H, t, J = 7.8 Hz, H17, H19), 7.86 (4 H,

d, $J = 6.5$ Hz, H16, H20), 8.06 (2 H, d, $J = 5.2$ Hz, H2), 8.17 (2 H, d, $J = 9.8$ Hz, H6), 8.32 (2 H, d, $J = 9.1$ Hz, H7), 8.38 (2 H, d, $J = 5.9$ Hz, H10), 10.09 (2 H, d, $J = 5.2$ Hz, H11). ^{13}C NMR (125 MHz, CD_2Cl_2, 303 K): δ 5.15 (*Me*CN), 126.23 (C2, C6), 126.63 (C7), 126.91 (Me*C*N), 127.66 (C10), 129.31 (C5, C8), 129.78 (C22, C23, C24, C25, C26), 130.22 (C18), 130.40 (C17, C19), 130.63 (C16, C20), 136.21 (C15, C21), 149.00, 149.89, 150.04, 150.49 (C4, C9, C13, C14), 153.04 (C3), 155.18 (C11). IR (KBr disk): υ 517, 573, 637, 702, 737, 766, 834, 851, 1030, 1152, 1223, 1262 (C−F), 1273, 1401, 1420, 1445, 1495, 1559, 1597, 1625, 2007 (C≡N), 3058 cm^{-1}. Anal. Calcd. for $C_{54}H_{38}F_6N_6O_6RuS_2 \cdot 2H_2O$: C, 54.86; H, 3.56; N, 7.11. Found: C, 55.18; H, 3.46; N, 6.39.

***trans*-[Ru(DIP)$_2$(MeOH)$_2$][OTf]$_2$ (4).** This species was obtained by slow crystallization (approximately 1 month) by the diffusion of diethyl ether into a concentrated solution of $[Ru(DIP)_2(OTf)_2]$ in methanol. (Note: This complex slowly decomposes in a CH_2Cl_2 solution.) ^{1}H NMR (500 MHz, CD_2Cl_2, 303 K): δ 3.46 (s, Me), 7.69 (d, $J = 7.2$ Hz), 7.74 (t, $J = 7.3$ Hz), 7.83 (m), 8.19 (d, $J = 5.4$ Hz), 8.27 (s), 10.44 (d, $J = 5.4$ Hz).

[Ru(DIP)$_2$(Hcmbpy)][Cl]$_2$ (5). A solution of $[Ru(DIP)_2Cl_2] \cdot DMF \cdot H_2O$ (100 mg, 0.11 mmol), Hcmbpy (25 mg, 0.12 mmol), and NaOAc (25 mg, 0.30 mmol, 2.5 equiv) in methanol and water (50 mL, 4:1 v/v) was heated to reflux for 24 h, causing the solution to turn from purple to red. The reaction mixture was then cooled to room temperature; the solution volume was concentrated to approximately one-third by evaporation of the solvent, and the pH was adjusted to 1 by the addition of dilute hydrochloric acid. Addition of NaCl (sat) resulted in the precipitation of the product, which was filtered and washed with NaCl (sat). The residue was dissolved in methanol and filtered, and the solvent was removed by evaporation. The residue was dissolved in CH_2Cl_2 and filtered; the addition of benzene resulted in the precipitation of the product. This was filtered, washed with benzene and diethyl ether, then dried under vacuum to give the product (104 mg, 92%) as a microcrystalline red powder. ^{1}H NMR (500 MHz, CD_2Cl_2, 293 K): δ 7.83 (1 H, d, $J = 5.4$ Hz, H5′), 7.66 (21 H, m, H5, Ph), 7.83 (3 H, d, $J = 5.3$ Hz, H8, H8′, H12′), 7.86 (1 H, d, $J = 5.4$ Hz, H12′), 7.89 (1 H, d, $J = 5.7$ Hz, H6′), 7.97 (1 H, d, $J = 5.3$ Hz, H7′), 8.19 (1 H, d, $J = 5.5$ Hz, H6), 8.27 (4 H, m, H9, H9′, H10, H10′), 8.37 (1 H, d, $J = 5.4$ Hz, H11), 8.43 (1 H, d, $J = 5.4$ Hz, H11′), 8.45 (1 H, d, $J = 5.5$ Hz, H7), 8.64 (1 H, s, H3′), 9.18 (1 H, s, H3). ^{13}C NMR (125 MHz, CD_2Cl_2, 293 K): δ 21.68 (CH_3), 124.64 (C3), 125.80 (C3′), 126.54 (CH), 126.85 (CH), 126.94 (CH), 127.33 (CH), 127.86 (CH), 129.26 (C5′), 129.48 (quat), 129.63 (m, Ph_a), 130.20 (m, Ph_b), 135.92 (quat), 135.97 (quat), 136.06 (quat), 148.60 (quat), 148.81 (quat), 148.97 (quat), 149.03 (quat), 149.60 (quat), 149.69 (quat), 149.83 (quat), 151.18 (quat), 151.62 (C12), 151.75 (C6′), 152.01 (C6), 152.18 (C11), 152.59 (C11′), 153.14 (C7′), 157.34 (quat), 157.50 (quat), 167.17 (CO) ppm. IR (KBr disk): υ 702, 766, 833, 1019, 1082, 1227, 1360, 1416, 1480, 1493, 1557, 1621, 1717 (CO), 1974, 3029, 3056, 3401s cm^{-1}. Anal. Calcd. for $C_{60}H_{42}Cl_2N_6O_2Ru \cdot 5H_2O$: C, 63.16; H, 4.59; N, 7.37. Found: C, 63.19; H, 4.20; N, 7.41.

[Ru(DIP)$_2$(H$_2$dcbpy)][Cl]$_2$ (6). A solution of $[Ru(DIP)_2Cl_2] \cdot DMF \cdot H_2O$ (500 mg, 0.54 mmol), H_2dcbpy (147 mg, 0.60 mmol, 1.1 equiv), and NaOAc (350 mg, 4.27 mmol, 7.9 equiv) in methanol and water (50 mL, 4:1 v/v) was heated to reflux for 24 h. The reaction mixture was then cooled to room temperature, and the pH was adjusted to 1 by the addition of dilute hydrochloric acid with vigorous stirring. The solution volume was then concentrated to approximately one-third by evaporation of the solvent. Addition of NaCl (sat) resulted in the precipitation of the product, which was filtered and washed with CH_2Cl_2. The precipitate was dissolved in ethanol and filtered, and the solvent was removed by evaporation. The residue was further washed with CH_2Cl_2 and diethyl ether to give the product (557 mg, 96%) as a microcrystalline dark red powder. ^{1}H NMR (500 MHz, MeOD-d_4, 300 K): δ 7.62−7.71 (20 H, m, Ph), 7.73 (2 H, d, $J = 5.0$ Hz, H18), 7.87 (2 H, d, $J = 5.5$ Hz, H9), 7.96 (2 H, dd, $J = 6.0$, 1.0 Hz, H5), 8.20 (2 H, d, $J = 5.5$ Hz, H6), 8.22 (2 H, d, $J = 5.5$ Hz, H19), 8.31 (4 H, m, H15, H16), 8.40 (4 H, d, $J = 5.5$ Hz, H8), 9.26 (2 H, d, $J = 0.5$ Hz, H3). ^{13}C NMR (100 MHz, MeOD-d_4, 300 K): δ 125.2 (C3), 127.5 (C15, C16), 127.8 (C9, C18), 128.2 (C5), 130.3 (m, Ph), 131.0−131.1 (m, Ph), 137.0 (C10, C17), 141.0 (C4), 149.4 (s, ring-fused C), 149.6 (s, ring-fused C), 151.3 (s, ring-fused C), 151.4, (s, ring-fused C), 153.1 (C19), 153.5 (C8), 154.2 (C6), 159.5 (C2), 166.0 (COOH). IR (KBr disk): υ 627, 664, 702, 737, 766, 833, 853, 1026, 1125, 1134, 1225, 1264, 1300, 1316, 1401, 1416, 1443, 1493, 1555, 1596, 1623, 1719 (CO), 3066, 3392(s) cm^{-1}. Anal. Calcd. for $C_{60}H_{40}Cl_2N_6O_4Ru \cdot {}^5/_2H_2O \cdot {}^1/_2CH_2Cl_2$: C, 62.19; H, 3.97; N, 7.19. Found: C, 61.92; H, 3.98; N, 7.20.

Computational Details

Calculations were performed with the GAUSSIAN 03 series of programs.[16] Density functional theory (DFT)[17] was applied for two model complexes (in which the phenyl substituents on the phenanthroline ligands were replaced by H atoms) with the B3PW91 functional.[18] The basis set for the ruthenium atom was that associated with the pseudo potential, with a standard double-ζ LANL2DZ contraction[19] completed by a set of polarization *f* functions (441/3111/311/1).[20] Geometry optimizations on the model complexes were performed with the 6-31+G* basis for P, S, and Cl atoms and with 6-31G* for H, C, N, and O atoms. The stationary points were characterized by full vibration frequency calculations. QM/MM optimizations of real complexes were performed at the ONIOM (B3PW91:UFF) level with the phenyl substituents in the MM part.[21] The QM part was treated at the DFT-B3PW91 level with the basis set used for the optimization of the model complexes (see above), and the UFF force field was used for the MM part.[22] Finally, DFT-B3PW91 single-point calculations were performed on the optimized structures (B3PW91//B3PW91:UFF calculations) using the same basis sets.

(16) Frisch, M. J.; Trucks, G. W.; Schlegel, H. B.; Scuseria, G. E.; Robb, M. A.; Cheeseman, J. R.; Montgomery, J. A., Jr.; Vreven, T.; Kudin, K. N.; Burant, J. C.; Millam, J. M.; Iyengar, S. S.; Tomasi, J.; Barone, V.; Mennucci, B.; Cossi, M.; Scalmani, G.; Rega, N.; Petersson, G. A.; Nakatsuji, H.; Hada, M.; Ehara, M.; Toyota, K.; Fukuda, R.; Hasegawa, J.; Ishida, M.; Nakajima, T.; Honda, Y.; Kitao, O.; Nakai, H.; Klene, M.; Li, X.; Knox, J. E.; Hratchian, H. P.; Cross, J. B.; Adamo, C.; Jaramillo, J.; Gomperts, R.; Stratmann, R. E.; Yazyev, O.; Austin, A. J.; Cammi, R.; Pomelli, C.; Ochterski, J. W.; Ayala, P. Y.; Morokuma, K.; Voth, G. A.; Salvador, P.; Dannenberg, J. J.; Zakrzewski, V. G.; Dapprich, S.; Daniels, A. D.; Strain, M. C.; Farkas, O.; Malick, D. K.; Rabuck, A. D.; Raghavachari, K.; Foresman, J. B.; Ortiz, J. V.; Cui, Q.; Baboul, A. G.; Clifford, S.; Cioslowski, J.; Stefanov, B. B.; Liu, G.; Liashenko, A.; Piskorz, P.; Komaromi, I.; Martin, R. L.; Fox, D. J.; Keith, T.; Al-Laham, M. A.; Peng, C. Y.; Nanayakkara, A.; Challacombe, M.; Gill, P. M. W.; Johnson, B.; Chen, W.; Wong, M. W.; Gonzalez, C.; Pople, J. A. *Guassian03*, revision B.04; Gaussian, Inc.: Pittsburgh, PA, 2003.

(17) (a) Ziegler, T. *Chem. Rev.* **1991**, *91*, 651−667. (b) Parr, R. G.; Yang, W. *DFT*; Oxford University Press: Oxford, U.K., 1989.

(18) Becke, A. D. *J. Chem. Phys.* **1993**, *98*, 5648−5652.

(19) Hay, P. J.; Wadt, W. R. *J. Chem. Phys.* **1985**, *82*, 299−310.

(20) Ehlers, A.; Böhme, M.; Dapprich, S.; Gobbi, A.; Höllwarth, A.; Jonas, V.; Köhler, K. F.; Stegmann, R.; Veldkamp, A.; Frenking, G. *Chem. Phys. Lett.* **1993**, *208*, 111−114.

(21) Svensson, M.; Humbel, S.; Froese, R. D. J.; Matsubara, T.; Sieber, S.; Morokuma, K. J. *J. Phys. Chem.* **1996**, *100*, 19357−19363.

(22) Rappé, A. K.; Casewitt, C. J.; Colwell, K. S.; Goddard, W. A.; Skiff, W. M. *J. Am. Chem. Soc.* **1992**, *114*, 10024−10035.

X-ray Molecular Structure of *trans*-[Ru(DIP)$_2$(MeOH)$_2$][OTf]$_2$ (4). The selected crystal was protected by paratone oil and Araldite and then mounted on top of a glass rod. Data were collected at 100 K on a Nonius KappaCCD diffractometer with graphite-monochromated Mo Kα radiation. The Nonius Supergui program package was used for cell refinement and data collection. The structure was solved by direct methods and subsequent difference Fourier treatment and refined by full-matrix least-squares on *F* using programs of the PC version of CRYSTALS.[23] The asymmetric unit contained half a molecule of the ruthenium complex and two CF_3SO_3 anions disordered over two positions with a 0.50:0.50 occupancy ratio. All non-CF_3SO_3 molecules and non-hydrogen atoms were refined anisotropically. Hydrogen atoms were introduced in calculated positions in the last refinements and were allocated an over all refinable isotropic thermal parameter.

Acknowledgment. H.A. thanks CNRS for providing J.B.W. a CNRS postdoctoral stipend. The authors thank Dr. M. N. Rager for technical assistance in NMR as well as the Université Pierre et Marie Curie and CNRS for supporting this work. IDRIS is acknowledged for providing computing facilities.

Supporting Information Available: X-ray crystallographic files in CIF format for the structure determination of **4**; Cartesian coordinates and views for computed structures cis and trans of **4**. This material is available free of charge via the Internet at http://pubs.acs.org.

IC0601236

(23) Watkin, D. J.; Prout, C. K.; Carruthers, R. J.; Betteridge, P. W. *CRYSTALS*; Oxford University: Oxford, U.K., 1996; Issue 10.